Acta Pharmaceutica Sinica B 2021;11(7):1914–1930

Chinese Pharmaceutical Association
Institute of Materia Medica, Chinese Academy of Medical Sciences

Acta Pharmaceutica Sinica B

www.elsevier.com/locate/apsb
www.sciencedirect.com

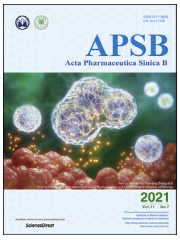

ORIGINAL ARTICLE

Inhibition of LIM kinase reduces contraction and proliferation in bladder smooth muscle

Qingfeng Yu[a,†], Chengjie Wu[a,†], Yeda Chen[a,†], Bingsheng Li[b,†], Ruixiao Wang[b], Ru Huang[b], Xuechun Li[a], Di Gu[a], Xiaolong Wang[b], Xiaolu Duan[a], Shujue Li[a], Yang Liu[a], Wenqi Wu[a], Martin Hennenberg[b], Guohua Zeng[a,*]

[a]*Department of Urology and Guangdong Key Laboratory of Urology, the First Affiliated Hospital of Guangzhou Medical University, Guangzhou 510230, China*
[b]*Department of Urology, University Hospital, LMU Munich, Munich 81377, Germany*

Received 28 July 2020; received in revised form 17 October 2020; accepted 3 November 2020

KEY WORDS

LIMK;
Cofilin phosphorylation;
Overactive bladder (OAB);
Lower urinary tract symptoms (LUTS);
Bladder smooth muscle contraction

Abstract Overactive bladder (OAB) is the most bothersome symptom in lower urinary tract symptoms (LUTS). Current pharmacologic treatment aims to inhibit detrusor contraction; however, shows unsatisfied efficacy and high discontinuation rate. LIM kinases (LIMKs) promote smooth muscle contraction in the prostate; however, their function in the bladder smooth muscle remains unclear. Here, we studied effects of the LIMK inhibitors on bladder smooth muscle contraction and proliferation both *in vitro* and *in vivo* experiments. Bladder expressions of LIMKs are elevated in OAB rat detrusor tissues. Two LIMK inhibitors, SR7826 and LIMKi3, inhibit contraction of human detrusor strip, and cause actin filament breakdown, as well as cell proliferation reduction in cultured human bladder smooth muscle cells (HBSMCs), paralleled by reduced cofilin phosphorylation. Silencing of *LIMK1* and *LIMK2* in HBSMCs resulted in breakdown of actin filaments and decreased cell proliferation. Treatment with SR7826 or LIMKi3 decreased micturition frequency and bladder detrusor hypertrophy in rats with bladder outlet

Abbreviations: 4E-BP1, 4E-binding protein 1; ADF, actin depolymerizing factors; BOO, bladder outlet obstruction; BPH, benign prostatic hyperplasia; CCK-8, Cell Counting Kit-8; Ct, number of cycles; DMSO, dimethyl sulfoxide; EdU, 5-ethynyl-2′-deoxyuridine; GAPDH, glyceraldehyde 3-phosphate dehydrogenase; H&E, hematoxylin and eosin; HBSMCs, human bladder smooth muscle cells; HRP, horseradish peroxidase; LIMKs, LIM kinases; LUTS, lower urinary tract symptoms; MLC, myosin light chain; MW, molecular weight; MYPT1, myosin-binding subunit; OAB, overactive bladder; PCNA, proliferating cell nuclear antigen; RT-qPCR, reverse transcription and quantitative polymerase chain reaction; siRNA, small interfering RNA; STK16, serine/threonine kinase 16; TESK1, testicular protein kinase 1; TXA2, thromboxane A2; WST-8, 2-(2-methoxy-4-nitrophenyl)-3-(4-nitrophenyl)-5-(2,4-disulfophenyl)-2*H*-tetrazolium monosodium salt.

*Corresponding author. Tel.: +86 20 34294165.
E-mail address: gzgyzgh@vip.sina.com (Guohua Zeng).
[†]These authors made equal contributions to this work.

Peer review under responsibility of Chinese Pharmaceutical Association and Institute of Materia Medica, Chinese Academy of Medical Sciences.

https://doi.org/10.1016/j.apsb.2021.01.005

obstruction. Our study suggests that LIMKs may promote contraction and proliferation in the bladder smooth muscle, which could be inhibited by small molecule LIMK inhibitors. LIMK inhibitors could be a potential therapeutic strategy for OAB- related LUTS.

1. Introduction

In lower urinary tract symptoms (LUTS), storage symptoms caused by overactive bladder (OAB) are the most bothersome and embarrassing[1], as these symptoms may increase the risk of falls and injuries[2,3], reduce the sleep and life quality, and even affect the health of partners[4], which are also chief complaint of patients searching medical care for LUTS. A prevalence study indicated that OAB affects 17% of the population, and increased to over 30% among those ≥65 years[5], as the demographic changes in the elderly population, it is estimated that the economic burden of OAB will increase to at least $65.9 billion in the United States in 2020[6].

Spontaneous and exaggerated contractions in bladder smooth muscle, which referred to as detrusor overactivity (DO), are the main contributor to the symptoms of OAB[7]. Therefore, the current therapeutic target for storage symptoms and OAB focuses on detrusor smooth muscle contraction[8]. Although the mechanism of spontaneous detrusor contractions is still mostly unclear, the muscarinic receptor antagonists have shown effect on improving storage symptoms by inhibiting the detrusor contraction, and has been widely used in the clinical practice as the first treatment option[9]. However, due to the limited efficacy and unbalanced side effects, high discontinuation rats were observed to be up to 30% after 12 weeks after the first prescription, and increase to as high as 90% after one year[10]. Although β_3-adrenoceptor agonists are recommended as an alternative option for treating storage symptoms[8], increasing evidences are indicating that their efficacy do not exceed the muscarinic receptor antagonists, moreover, the long-term effect still remains inadequate[11]. Several studies have revealed that noncholinergic agonists, for example, thromboxane A_2, prostanoids, and endothelin-1 may also cause detrusor contractions[12–14], this may partially explain the unsatisfied efficacy of anticholinergics and β_3-adrenoceptor agonists. Consequently, due to the unsatisfied efficacy and high discontinuation rates of the available pharmacological options, novel treatment strategies become more warranted than ever, and a more precise understanding of detrusor contraction is highly required.

Smooth muscle contraction requires actin reorganization[15]. LIM domain kinases (LIMKs) are serine/threonine kinases, which occur in two isoforms (LIMK1 and LIMK2). LIMKs could promote actin polymerization through phosphorylation of the actin depolymerizing factors (ADF)/cofilin, and subsequently cause filament organization and stress fibre formation[16]. Recently, two LIMK inhibitors, SR7826 and LIMKi3, have been reported to inhibit human prostate smooth muscle contractions[17]; however, their effects on detrusor contractions are still unclear. Here, we examined the effects of these inhibitors on detrusor contraction and proliferation.

2. Materials and methods

2.1. Sample collection

Human detrusor tissues and prostate tissues were obtained from patients ($n = 78$) undergoing cystectomy for bladder cancer according to a previous described method[18]. Patients with previous bladder instillation therapy or pelvic radiotherapy were excluded. This study was performed in accordance with the Declaration of Helsinki of the World Medical Association, and has been approved by the ethics committee of the first affiliated hospital of Guangzhou Medical University (Guangzhou, China). Informed consent was obtained from all patients. Organ bath studies and phosphorylation analyses were performed immediately after sampling, while samples for other molecular analyses were shock-frozen in liquid nitrogen and stored at −80 °C.

2.2. RT-qPCR

RNA from frozen detrusor tissues, prostate tissues or cells was isolated according to a previous described method[17]. The specific primers were as indicated: *LIMK1*: 5′-TTCTTGCGGTCTGGCTTC-3′ (forward) and 5′- TGGTGGTGGCTGACTTCG-3′ (reverse). *LIMK2*: 5′-CTTTGCCCGTGGCTTTGT-3′ (forward) and 5′-CCGCTCAGAATCCCTTCG-3′ (reverse). Primers set for *GAPDH* was 5′-CCAGGTGGTCTCCTCTGACTTC-3′ (forward) and 5′-GTGGTCGTTGAGGGCAATG-3′ (reverse).

2.3. Western blot analysis

Proteins of cells, and frozen prostate and detrusor tissues were isolated according to a previously described method[19]. Primary antibodies for Western blot analyses included rabbit anti-phospho-cofilin (Ser3; 77G2, #3313), rabbit cofilin (D3F9, #5175S), rabbit anti-phospho-LIMK1 (Thr508)/LIMK2 (Thr505, #3841), rabbit anti-myosin-binding subunit (MYPT1, #2634), rabbit anti-myosin light chain (MLC) 2 (#3672), rabbit anti-phospho-myosin light chain 2 (Ser19; #3671), rabbit anti-phospho-eukaryotic translation initiation factor 4E-binding protein 1 (4E-BP1, Thr37/46; #9459), rabbit anti-phospho-4E-BP1 (Ser65; #9451), rabbit anti-4E-BP1 (#9452) (Cell Signaling Technology, USA), mouse anti-calponin 1/2/3 (sc-136987), mouse anti-vimentin (sc-6260), mouse monoclonal anti-GAPDH (sc-32233) (Santa Cruz Biotechnology, Santa Cruz, CA, USA), rabbit anti-LIMK1 (ab81046), rabbit anti-LIMK2 (ab45165) (Abcam, Cambridge, UK). Detection was

continued using secondary antibodies IRDye® 800CW goat anti-mouse (or rabbit) IgG and IRDye® 680RD goat anti-mouse (or rabbit) IgG (LI-COR). The bands were detected by using Odyssey® Clx Imaging Systems and quantified with respect to GAPDH using ImageJ software.

2.4. Fluorescence staining

Human detrusor specimens, embedded in optimal cutting temperature compound, were snap-frozen in liquid nitrogen and kept at −80 °C. Sections were cut and labeled with the following primary antibodies: rabbit anti-LIMK1 antibody (ab81046), rabbit anti-LIMK2 (ab45165) (Abcam, Cambridge, UK), mouse anti-calponin 1/2/3 (sc-136987), mouse anti-vimentin (sc-6260) (Santa Cruz Biotechnology), rabbit anti-phospho-cofilin (Ser3; 77G2, #3313), rabbit cofilin (D3F9, #5175S) (Cell Signaling Technology). Binding sites were visualized using goat anti-mouse IgG H&L (Cy3®, ab97035), goat anti-rabbit IgG H&L (Cy5®, ab6564) (Abcam). Nuclei were counterstained with DAPI (Invitrogen, Camarillo, USA). Immunolabelled sections were analyzed using a laser microscope (IX73, Olympus, Tokyo, Japan). Control staining without primary antibodies did not yield any signals.

2.5. Tension measurements

Detrusor strips (6 mm × 3 mm × 3 mm) were isolated from human bladders and evaluated the contractions according to a previously described method[18]. Cumulative concentration−response curves for carbachol and acetylcholine (Sigma−Aldrich, St. Louis, MO, USA), U46619 (APExBIO, Huston, TX, USA), endothelin-1 (Tocris Bioscience, Bristol, UK) or frequency−response curves induced by electrical field stimulation (EFS) were evaluated after adding inhibitors or DMSO for controls. Effects of SR7826, LIMKi3 and Y27632 (a selective ROCK inhibitor) were evaluated in separate series of experiments, performing with corresponding controls from the same detrusor sample in each experiment. For the calculation of agonist- or EFS-induced contractions, percentage of KCl-induced contractions were used to express the tensions, as this corrects for different smooth muscle content in each strip.

2.6. Cell culture

Human bladder smooth muscle cells (HBSMCs) were purchased from ScienCell Research Laboratories (Cat. No. 4310, Carlsbad, CA, USA) and grown in smooth muscle cell medium (Cat. No. 1101; ScienCell, Carlsbad) at 37 °C with 5% CO_2. Before addition of SR7826 or LIMKi3, the medium was changed to a fetal calf serum and growth factor-free medium, while in the 5-ethynyl-2′-deoxyuridine (EdU) assay, cells were grown in a complete medium.

2.7. Phosphorylation studies

Tissues from each bladder were cut into several small strips (6 mm × 1 mm × 1 mm), which were then allocated to two samples (control and inhibitor, or control and agonist). Incubation of samples with inhibitors (SR7826, LIMKi3, or Y27632), agonists (carbachol, acetylcholine, U46629, eothelin-1) and solvent (DMSO or H_2O) was performed in 6-well plates filled with Krebs-Henseleit solution and kept at 37 °C under continuous shaking for 1 h. Following incubations, tissues were shock frozen with liquid nitrogen and subjected to Western blot analysis for p-cofilin, cofilin, phospho-LIMK, LIMK, phospho-MYPT1, MYPT1, phospho-4E-BP1, 4E-BP1, phospho-MLC, MLC, and GAPDH. Tissues incubated with Y27632 were subjected to Western blot analysis for phospho-MYPT1 and MYPT1. For phosphorylation analyses in HBSMCs, cells were grown in 10 mm dishes and treated with inhibitors or DMSO for 24 h before Western blot analysis.

2.8. Phalloidin staining

For fluorescence staining of polymerized actin with phalloidin, cells were plated on 6-well cell culture plate and covered with inhibitors or solvent (DMSO). Staining was performed using 200 nmol/L FITC-labelled phalloidin (Solarbio life sciences, Beijing, China) according to the manufacturer's instructions. Nuclei were counterstained with DAPI (Invitrogen). Labelled cells were analyzed using a fluorescence microscopy (IX73, Olympus).

2.9. Viability assay

Effects of LIMK inhibitors on viability of HBSMCs were assessed using the Cell Counting Kit-8 (CCK-8, Dojindo Laboratories, Kumamoto, Japan). Cells were grown in 96-well plates (5000 cells/well) for 24 h before the medium with inhibitors in different concentrations or solvent (DMSO) was refreshed. Subsequently, cells were grown for different time periods (24, 48 or 72 h). At the end of each period, 10 μL of 2-(2-methoxy-4-nitrophenyl)-3-(4-nitrophenyl)-5-(2,4-disulfophenyl)-2*H*-tetrazolium monosodium salt (WST-8) from CCK-8 was added, and absorbance in each well was measured at 450 nm after incubation for 2 h at 37 °C.

2.10. EdU proliferation assay

HBSMCs were plated on 24-well cell culture plate (100,000/well). After 24 h, cells were treated with inhibitors in different final concentrations or solvent (DMSO). After a further 24 h, the medium was changed to a 10 μmol/L 5-ethynyl-2′-deoxyuridine (EdU) solution medium containing inhibitors or solvent (DMSO) and incubated for another 24 h. Subsequently, cells were fixed with 4% paraformaldehyde. EdU incorporation was assessed using the EdU Cell Proliferation Assay Kit (Ribobio, Guangzhou, China). Counterstaining of all nuclei was performed with DAPI (Invitrogen). Cells were analyzed by a fluorescence microscopy (IX73, Olympus).

2.11. Silencing of LIMK1 and LIMK2 expressions

HBSMCs were transfected with scrambled siRNA, *LIMK1* siRNA 5′-GACCGGAUCUUGGAAAUCATT-3′ (forward) and 5′-UGAUUUCCAAGAUCCGGUCTT-3′ (reverse), or *LIMK2* siRNA 5′-GCCAGACACUUCAGCUGUUTT-3′ (forward) and 5′-AACAGCUGAAGUGUCUGGCTT-3′ (reverse). The *LIMK1*, *LIMK2*, and scrambled siRNAs were diluted in Opti-MEM containing Lipofectamine® 3000 (Thermo Fisher Scientific, Inc., Waltham, MA, USA). Cells were 60% confluent at the time of transfection, and incubated with transfection mixture for 48 h at 37 °C (5% CO_2) before the medium was replaced by normal smooth muscle cell culture medium. For RT-qPCR and Western blot analyses, cells were harvested 48 h after transfection. For phalloidin staining, cells were fixed and stained 48 h after

transfection. EdU was performed 24 h after transfection and incubated for an additional 24 h before incorporation.

2.12. Animal and bladder outlet obstruction model

Twenty male Sprague−Dawley rats (body weight 250−280 g) were purchased from Guangdong Medical Laboratory Animal Center, Guangzhou, China. All animal experiments were carried out in accordance with protocols approved by the Institutional Animal Care and Use Committee of the Guangzhou Medical University, Guangzhou, China. The rats were anesthetized by intraperitoneal injection with 3% pentobarbital sodium (35 mg/kg). The BOO rats were created using a previously described method[20]. In brief, after an incision on suprapubic midline was made, the prostatic urethra was isolated carefully to avoid jeopardize the seminal vesicles and ureters at the ureterovesical junction. A sterile metal bar in 1 mm outer diameter was placed on the prostatic urethral surface, and a 3-0 polypropylene suture was used to tie around both the prostatic urethra and the bar. After the suture was secured, the bar was removed, and the incision was closed. The rat in sham group received the same procedure except for the urethra ligation.

After surgery, 15 BOO rats were randomized to control (DMSO + saline), SR7826, or LIMKi3 treatment (both were 1 mg/kg·day) by intraperitoneal injection. The 5 rats in sham group received only DMSO + saline by intraperitoneal injection. Daily treatment was initiated at the second day of surgery and last for two weeks.

2.13. Urinary frequency measurement

Urinary frequency was measured by a previously described method[21]. Briefly, rats were placed in metabolic cages without access to water for 2 h. A piece of filter paper which was impregnated with saturated copper sulfate solution ($CuSO_4 \cdot 5H_2O$) and dehydrated at 140 °C for 2 h, was placed under the base of the cage. Urinary frequency was determined by the number of spots on the filter paper. Overlapping spots with defined edges were considered as separate urinations.

2.14. Histological and immunohistochemical staining

The bladder, lung, liver, and kidney of rats were fixed overnight in 4% paraformaldehyde, and embedded in paraffin blocks. For histopathologic evaluation, sections (4 μm) of lung, liver and kidney were stained with hematoxylin and eosin (H&E), and the bladder was stained with Masson trichrome. Immunohistochemistry of tissue section was performed to analyze the proliferation of smooth muscle cells. Sections were deparaffinized and subjected to heat in citrate buffer for antigen retrieval. After being blocked with 2% BSA, sections were incubated overnight at 4 °C in mouse anti-proliferating cell nuclear antigen (PCNA; #2586, Cell Signaling Technology), and subsequently the biotin-conjugated secondary antibody. Sections were incubated with enzyme conjugate horseradish peroxidase (HRP)-streptavidin and lightly counterstained with hematoxylin/eosin. ImageJ software was used to perform the quantitative digital image analysis.

2.15. Statistical analysis

Data are presented as mean ± standard error of mean (SEM) with the indicated number (n) of independent experiments. Multivariate analysis of variance and two-way analysis of variance were used for unpaired observations and were performed with SPSS version 23.0 (IBM SPSS Statistics, IBM Corp., Armonk, NY, USA). P values < 0.05 were considered statistically significant. All groups included in the statistical analyses were based on five or more patients in the case of organ bath experiments performed with human tissues. For the series of endothelin-1-induced contractions, it was obvious that no effect could be expected even after more than five experiments. Therefore, these series were stopped after three independent experiments, and no statistical tests were applied to the results. All groups being compared with each other by statistical tests showed identical group sizes, consequently, any statistical comparisons between groups of different sample sizes or between groups composed of tissues from different patients were not performed.

3. Results

3.1. LIMK and cofilin detection in human detrusor tissues and human bladder smooth muscle cells (HBSMCs)

Western blot analysis of detrusor, prostate tissue and HBSMCs revealed bands with sizes of the expected molecular weight (MW) of LIMK1, LIMK2 (both 72 kDa), and cofilin (19 kDa), while evident variations in band intensities between samples from different patients could be observed (Fig. 1A). Bands obtained from cells show similar intensity between samples from different cell groups (Fig. 1A). Bands for calponin and vimentin as markers for smooth muscle[22] and mesenchymal cells[23], respectively, were observed in all detrusor and prostate samples included to these analyses, despite varying intensities between samples from different patients (Fig. 1A). In HBSMCs, bands for calponin and vimentin were also observed with similar intensity for calponin, but varying intensity for vimentin between samples of different cell groups (Fig. 1A). The correlation coefficient resulting from analysis of assumed bands for LIMK1 indicates a possible correlation between detrusor and prostatic LIMK1 content ($R = 0.403$), but a week correlation of LIMK2 content ($R = 0.056$, Fig. 1A). Analysis by RT-PCR shows mRNA expression of *LIMK1* and *LIMK2* in human detrusor, prostate tissues and in HBSMCs, confirming their expression in tissues and cells (Fig. 1B).

Histological sections were prepared and stained from detrusor tissues from three different patients. Following fluorescence staining of sections with antibodies raised against LIMK1, LIMK2, cofilin, phospho-cofilin, calponin, and vimentin, immunoreactivities for LIMK1, LIMK2, cofilin, and phospho-cofilin were observed in smooth muscle cells (calponin-positive cells), but only to limited extent in mesenchymal tissue (vimentin-positive mesenchymal cells, Fig. 1C).

3.2. SR7826 and LIMKi3 inhibit detrusor contractions in vitro

Carbachol (0.1−1000 μmol/L) induced concentration-dependent contractions of detrusor strips, which were inhibited by SR7826 and LIMKi3 (both 1 μmol/L, Fig. 2A and B). For SR7826, inhibition was significant after multivariate analysis at 100, 300 and 1000 μmol/L carbachol (Fig. 2A), for LIMKi3, inhibition was significant at 1000 μmol/L carbachol (Fig. 2B).

Acetylcholine (0.1−1000 μmol/L) induced concentration-dependent contractions of detrusor strips, which were inhibited

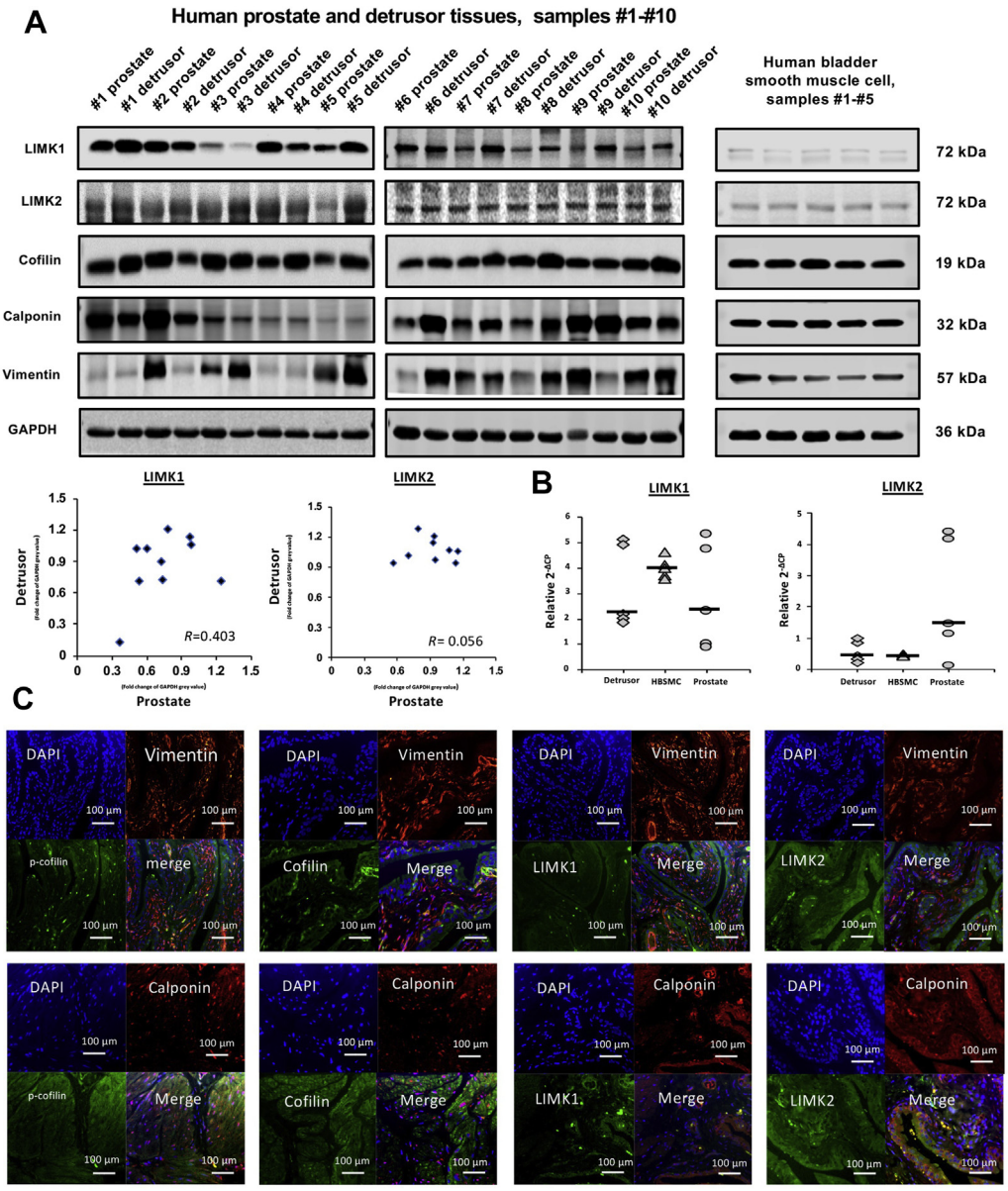

Figure 1 Detection of LIMK and cofilin in human bladder tissues and smooth muscle cells. Samples of prostate and bladder tissues, and HBSMCs were subjected to (A) Western blot analysis [prostate and detrusor tissues from patients ($n = 10$) or cells ($n = 5$) in independent experiments] or (B) RT-PCR [prostate and detrusor tissues from patients ($n = 10$) or cells ($n = 5$) in independent experiments]. Data in (A), bands for all samples included were shown with sizes matching the expected and indicated MWs of proteins. Bands were quantified and plotted in diagrams and subjected to Spearman's correlation analysis. Data in (B) are ΔΔCP values ($2^{-(\text{Cttarget}-\text{CtGAPDH}}$) normalized to each other and median values (bar). In (C), human bladder tissues were stained by immunofluorescence. Sections were double labelled with antibodies for LIMK1, LIMK2, cofilin, or p-cofilin. An antibody for calponin served as a marker for smooth muscle cells, and an antibody for vimentin as a marker for mesenchymal cells. The merged pictures indicate colocalization of target proteins. Shown are representative pictures from a series of tissues from $n = 3$ patients for each combination.

by SR7826 and LIMKi3 (both 1 μmol/L, Fig. 2C and D). For SR7826, inhibition was significant after multivariate analysis at 10, 30, 100 and 300 μmol/L acetylcholine (Fig. 2C), for LIMKi3, inhibition was significant at 100 and 300 μmol/L acetylcholine (Fig. 2D).

Electric field stimulation (EFS) (2−32 Hz) induced frequency-dependent contractions of detrusor strips, which were inhibited by SR7826 and LIMKi3 (both 1 μmol/L, Fig. 2E and F). For SR7826, inhibition was significant after multivariate analysis at 32 Hz (Fig. 2E), for LIMKi3, inhibition was significant at 8, 16, and 32 Hz (Fig. 2F).

The thromboxane A_2 analog, U46619 (0.1−30 μmol/L), induced concentration-dependent contractions of detrusor strips, which were inhibited by SR7826 and LIMKi3 (both 1 μmol/L,

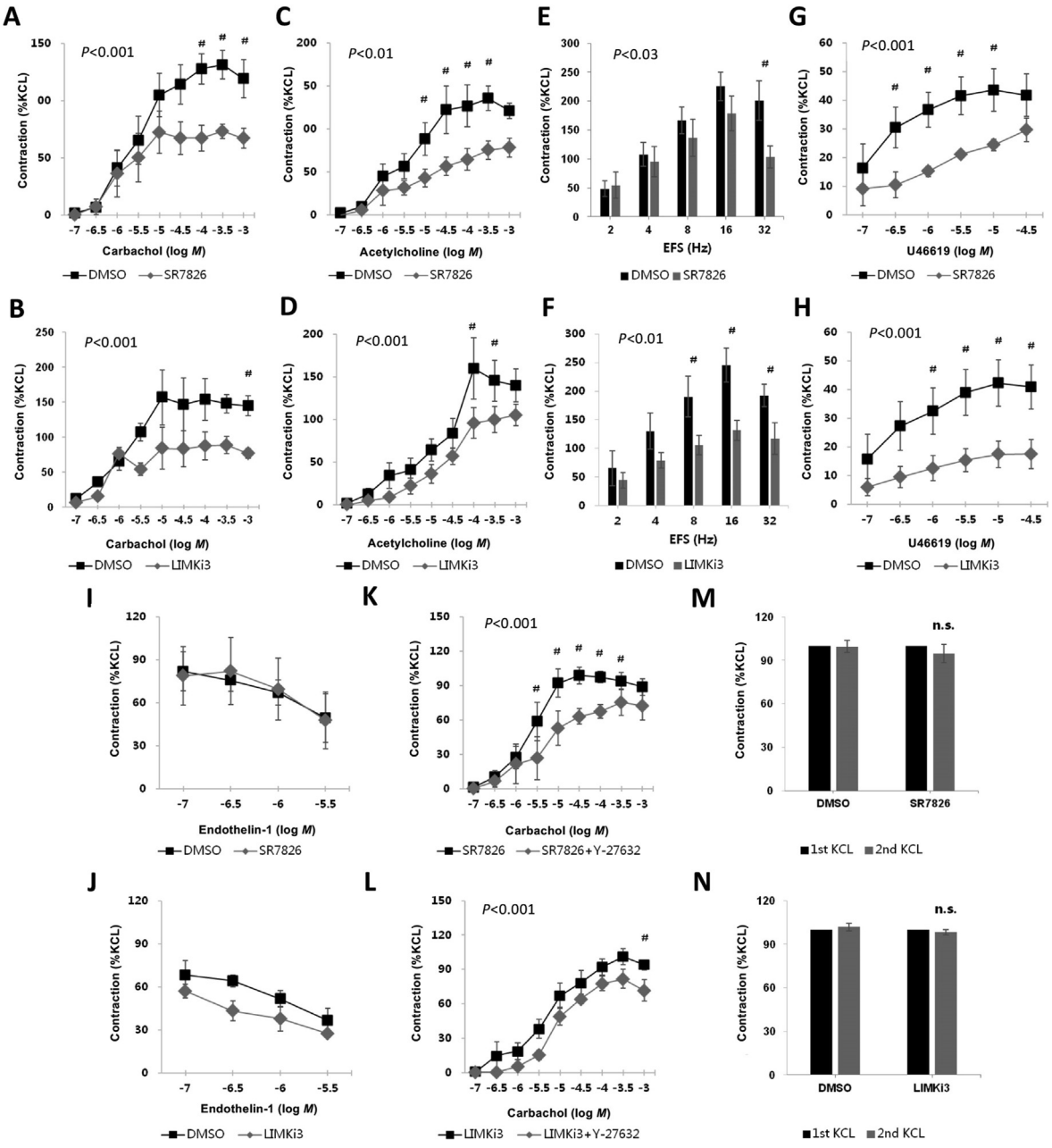

Figure 2 Effects of SR7826 and LIMKi3 on agonists-, KCl-, and EFS-induced contractions of human detrusor strips. Effects of the LIMK inhibitors SR7826 or LIMKi3 (both at 1 μmol/L) on detrusor contractions were compared with corresponding controls (solvent: DMSO) in separate sets of experiments. Samples from the same tissue (each patient) were used for the inhibitor and control groups, therefore, both groups in each diagram had identical group sizes. To eliminate heterogeneities due to individual variations or different smooth muscle content in each strip (as shown in Fig. 1), tensions were expressed as percentage of contraction (%) induced by high molar KCl, which were assessed before application of inhibitors or solvent. Data are mean ± SEM from a series of tissues from patients (A) $n = 5$ for carbachol/SR7826, (B) $n = 6$ for carbachol/LIMKi3, (C) $n = 5$ for acetylcholine/SR7826 and (D) $n = 5$ for acetylcholine/LIMKi3, (E) $n = 8$ for EFS/SR7826 and (F) $n = 6$ for EFS/LIMKi3, (G) $n = 5$ for U46619/SR7826 and (H) $n = 5$ for U46619/LIMKi3, or (I) $n = 3$ for endothelin-1/SR7826 and (J) $n = 3$ for endothelin-1/LIMKi3. In (K) and (L), Effects of SR7826 or LIMKi3 (both at 1 μmol/L) on contractions were tested in combination with the selective Rho kinase inhibitor Y27632 (30 μmol/L). Contractions were compared in the presence of SR7826 or LIMKi3 alone or in the presence of a combination of SR7826 or LIMKi3 with Y27632. Data are mean ± SEM from a series of tissues from patients (K) $n = 6$ for SR7826 *versus* SR7825+Y27632 and (L) $n = 5$ for LIMKi3 *versus* LIMKi3+Y27632. In (M) and (N), both were $n = 5$ patients. KCl-induced contractions of detrusor stripes in an organ bath were first assessed ("1st KCl"), and again after incubation of LIMK inhibitors (1 μmol/L) or solvent (DMSO; "2nd KCl"). Inhibitor and solvent were not washout before the 2nd KCl. Contraction values induced by 2nd KCl were calculated as percantage of the values induced by 1st KCl. $^{\#}P < 0.05$ for control *vs*. inhibitor. n.s., not significant *vs*. corresponding first KCl, or *vs.* second KCl in control.

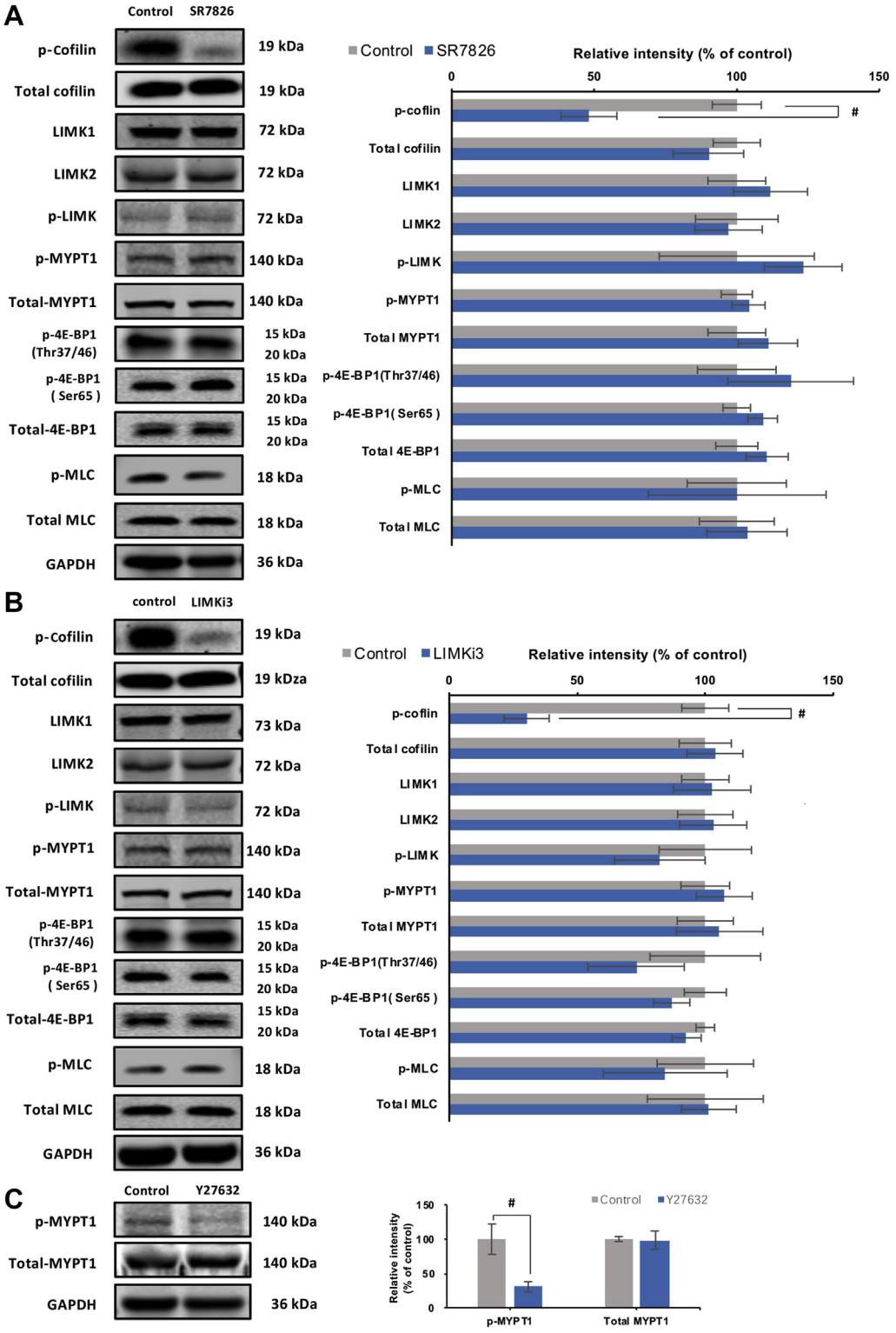

Figure 3 Effects of SR7826, LIMKi3 and Y27632 on phosphorylation in human bladder detrusor tissues. In separate series of experiments, detrusor tissues were incubated with (A) SR7826 (1 μmol/L, 1 h) or DMSO (control), or with (B) LIMKi3 (1 μmol/L, 1 h) or DMSO (control), or with (C) Y27632 (30 μmol/L, 1 h) or DMSO. In the series of SR7826 and DMSO, or LIMKi3 and DMSO, Western blot analyses using site- and phospho-specific antibodies were subsequently performed to compare the phosphorylation states of cofilin, LIMK and MYPT1 (threonine 696), 4E-BP1 (threonine 37/46, serine 65) and MLC between inhibitor and control groups. In the series of Y27632 and DMSO, Western blot using site- and phospho-specific antibodies was subsequently performed to compare the phosphorylation states of MYPT1 (threonine 696). Values for each sample were calculated as fold of the content of GAPDH and normalized to the mean of the corresponding control group. Data are mean ± SEM from a series of tissues from $n = 7$ (SR7826), $n = 7$ (LIMKi3), and $n = 5$ (Y27632). $^{\#}P < 0.05$ for control *vs*. inhibitor.

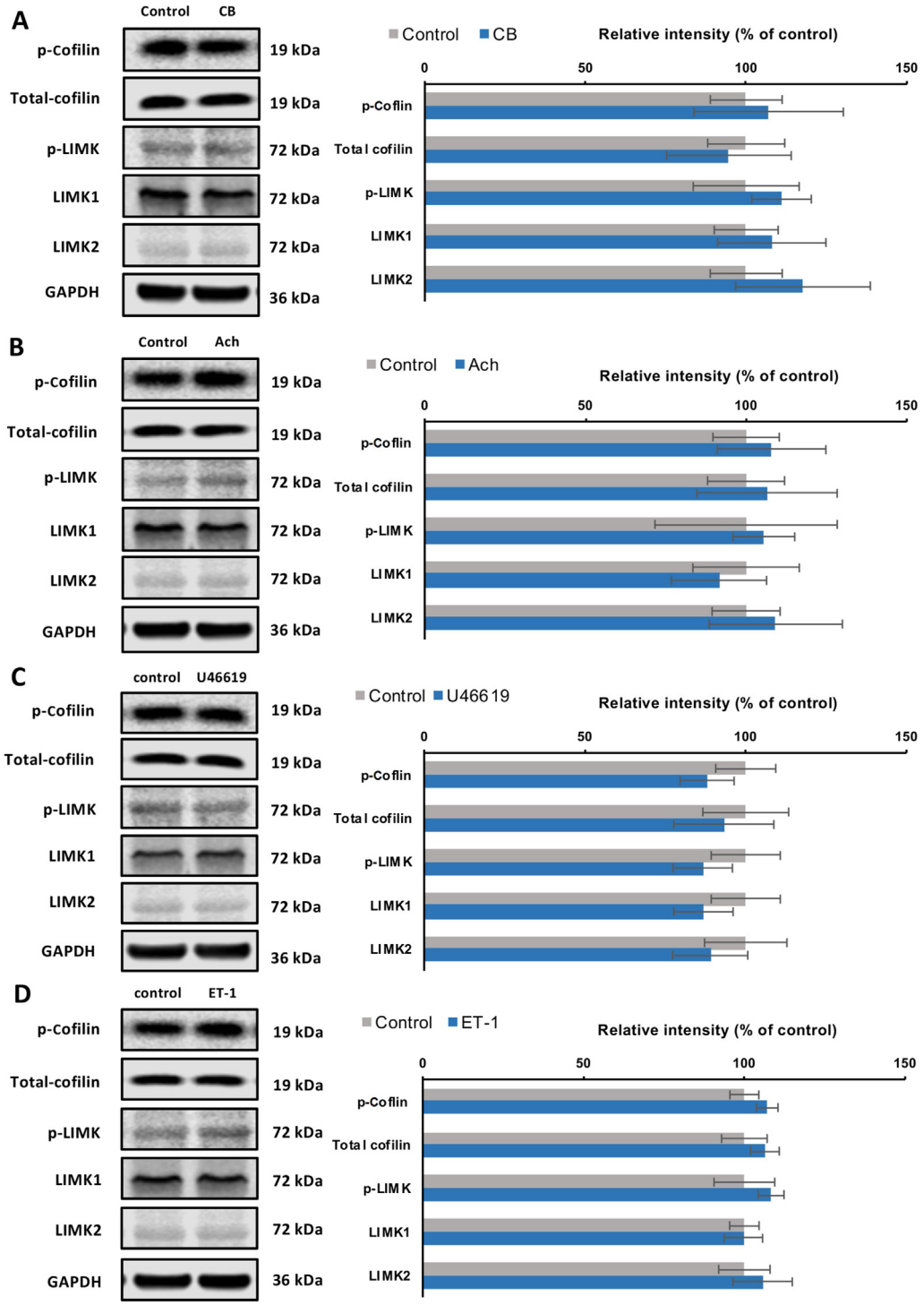

Figure 4 Effects of contractile stimuli on LIMK and cofilin phosphorylation in human bladder detrusor tissues. In separate series of experiments, detrusor tissues were incubated with (A) carbachol (CB, 1000 μmol/L), or with (B) acetylcholine (ACh, 1000 μmol/L), or with (C) U46619 (30 μmol/L), or with (D) endothelin-1 (ET-1, 3 μmol/L) for 1 h, or with solvent (H_2O for carbachol, acetylcholine, endthelin-1, and ethanol for U46619) as required. Western blot analyses using site- and phospho-specific antibodies were subsequently performed to compare the phosphorylation states of cofilin and LIMK. Values for each sample were calculated as fold of the content of GAPDH and normalized to the mean of the corresponding control group. Data are mean ± SEM from a series of tissues ($n = 5$) for each agonist experiment serial. $^{\#}P < 0.05$ for control *vs*. agonist.

Fig. 2G and H). For SR7826, inhibition was significant after multivariate analysis at 0.3, 1, 3 and 10 μmol/L U46619 (Fig. 2G), for LIMKi3, inhibition was significant at 1, 3, 10, and 30 μmol/L U46619 (Fig. 2H).

Endothelin-1 (0.1−3 μmol/L) induced concentration-dependent contractions of detrusor strips. However, the contractions induced by endothelin-1 were neither inhibited by SR7826, nor by LIMKi3 (both 1 μmol/L, Fig. 2I and J).

Carbachol-induced contractions of detrusor strips were induced after addition of SR7826 (1 μmol/L) or LIMKi3, alone or of a combination containing SR7826 (1 μmol/L) and Y27632 (30 μmol/L) or LIMKi3 (1 μmol/L) and Y27632 (30 μmol/L, Fig. 2K and L). Contractions in the presence of SR7826 were further significantly inhibited by Y27632 at 10, 30 and 100 μmol/L carbachol (Fig. 2K, $P < 0.05$), and contraction in the presence of LIMKi3 was further significantly inhibited by Y27632 at 1000 μmol/L carbachol (Fig. 2L, $P < 0.05$).

Two-way ANOVA was performed to compare the whole inhibitor and control groups (solvent of inhibitors: DMSO), and confirmed the significant inhibition of agonist-induced contractions by SR7826 and LIMKi3 ($P < 0.05$). In the SR7826/LIMKi3 and Y27632 series, two-way ANOVA was performed to compare the SR7826/LIMKi3 with the SR7826/LIMKi3+Y27632 groups, and confirmed the significant additional inhibitory effect of Y27632 on residual contractions ($P < 0.05$).

To assess possible contributions of toxic effects to the inhibitions of agonist-induced contractions, we tested the effects of SR7826 and LIMKi3 on high molar KCl-induced contractions of detrusor tissues. Contractions by high molar KCl were induced in an organ bath before incubation with SR7826 (1 μmol/L) or solvent (DMSO), or with LIMKi3 (1 μmol/L) or solvent (DMSO), and again after incubation with LIMK inhibitors or solvent. Contractions induced by KCl were only slightly, but not significantly attenuated compared to contractions induced by KCl before incubation with SR7826 (Fig. 2M) or LIMKi3 (Fig. 2N).

3.3. SR7826 and LIMKi3 reduce cofilin phosphorylation in detrusor tissues

Using site- and phospho-specific antibodies, phosphorylated proteins and their total content were semiquantitatively compared by Western blot analysis between detrusor tissues incubated for 1 h either by SR7826 or LIMKi3 (both at 1 μmol/L) and solvent-incubated controls (Fig. 3A). The content of phospho-cofilin (serine-3) in detrusor tissues was reduced by SR7826 and LIMKi3 (Fig. 3A). SR7826 significantly reduced the phospho-cofilin content by 52.9 ± 9.8% ($P < 0.05$), while LIMKi3 reduced by 69.3 ± 8.8% ($P < 0.05$). In contrast, the contents of total cofilin, phospho-LIMK (threonine-508/505), LIMK1, LIMK2, phospho-MYPT1 (threonine-696), MYPT1, phospho-4E-BP1 (threonine-37/46 and serine-65), 4E-BP1, phospho-MLC, and MLC remained unchanged by either SR7826 or LIMKi3 (Fig. 3A).

To confirm that threonine-696 phosphorylation of MYPT1 in detrusor tissues can be affected by Rho kinase inhibition, the effects of the Rho kinase inhibitor Y27632 on phosphorylation of this position was examined by Western blot analysis. Y27632 significantly reduced the content of threonine-696-phosphorylated MYPT1 by 47.5 ± 7.5% ($P < 0.05$), but did not change the contents of total MYPT1 (Fig. 3B).

Effects of different contractile stimuli on the content of phospho-cofilin, cofilin, phospho-LIMK, LIMK1, LIMK2, were examined by Western blot analysis (Fig. 4). Detrusor tissues were incubated with either carbachol or acetylcholine (both 1000 μmol/L) for 1 h; however, no change in the content of phospho-cofilin, cofilin, phospho-LIMK, LIMK1, or LIMK2 was detected (Fig. 4A and B). Similarly, no change in the content of these proteins was found when detrusor tissues were incubated with non-muscarinic receptor agonists, including U46619 (30 μmol/L, 1 h; Fig. 4C) or endothelin-1 (3 μmol/L, 1 h; Fig. 4D).

3.4. SR7826 and LIMKi3 reduce cofilin phosphorylation in HBSMCs

Using site-specific and phospho-specific antibodies, phosphorylated proteins and their total content were semiquantitatively compared by Western blot analyses between HBSMCs incubated for 24 h either by SR7826 or LIMKi3 (5 μmol/L) or solvent (Fig. 5). The content of phospho-cofilin (serine-3) in HBSMCs was reduced by SR7826 and LIMKi3 (Fig. 5). SR7826 and LIMKi3 significantly reduced the phospho-cofilin content by 36.8 ± 7.0% and 60.7 ± 6.6% (both were $P < 0.05$), respectively. In contrast, the contents of total cofilin, phospho-LIMK (threonine-508/505), LIMK1, LIMK2, phospho-MYPT1 (threonine-696), MYPT1, phospho-4E-BP1 (threonine-37/46 and serine-65), 4E-BP1, MLC remained unchanged by either SR7826 or LIMKi3 (Fig. 5). Preliminary experiments did not provide an informative basis that incubation with inhibitors in 1 μmol/L results in changes in cofilin or LIMK phosphorylation (data not shown). Therefore, these experiments in HBSMCs were performed using the concentration of 5 μmol/L.

3.5. SR7826 and LIMKi3 break down the actin cytoskeleton and inhibit proliferation in HBSMCs

Actin organization in HBSMCs was visualized by phalloidin staining. In cells of the solvent-treated control group, actin was organized to long filaments in most of the cells, and filamentous protrusions of these cells overlapped each other (Fig. 6A and B). Treatment with either SR7826 or LIMKi3 for 24 h showed concentration-dependent effects. Treatment with 5 μmol/L SR7826 or LIMKi3 reduced the length of filaments, although cells with an actin organization similar to controls were still visible but obviously less (Fig. 6A). Treatment with 10 μmol/L SR7826 or LIMKi3 caused extensive breakdown of actin organization, including shortening of filaments in most of the cells. The phalloidin-stained area of cells was reduced by 16.0 ± 3.5% (SR7826, 5 μmol/L) and 19.9 ± 3.6% (SR7826, 10 μmol/L), 22.3 ± 2.4% (LIMKi3, 5 μmol/L) and 29.2 ± 2.6% (LIMKi3, 10 μmol/L) compared with controls, respectively ($P < 0.05$, Fig. 6A).

In a viability assay, SR7826 and LIMKi3 showed concentration- and time-dependent effects on HBSMCs. At a concentration of 1 μmol/L, both SR7826 and LIMKi3 showed slight effects on viability after 24, 48 or 72 h of treatment (Fig. 6C and D). At concentrations of 5 and 10 μmol/L, both inhibitors markedly reduced viability in cells after 48 h of treatment (Fig. 6C and D). Therefore, following proliferation tests in HBSMCs were conducted using concentrations of 5 and 10 μmol/L under treatment for 48 h.

In the EdU assay, both SR7826 and LIMKi3 resulted in concentration-dependent reductions of the proliferation rate, amounting to 39.3 ± 2.9% (SR7826, 5 μmol/L) and 51.5 ± 2.5% (SR7826, 10 μmol/L), and 29.5 ± 4.7% (LIMKi3, 5 μmol/L) and 57.8 ± 1.7% (LIMKi3, 10 μmol/L) decrease of the proliferation rate compared with control cells, respectively ($P < 0.05$, Fig. 6E).

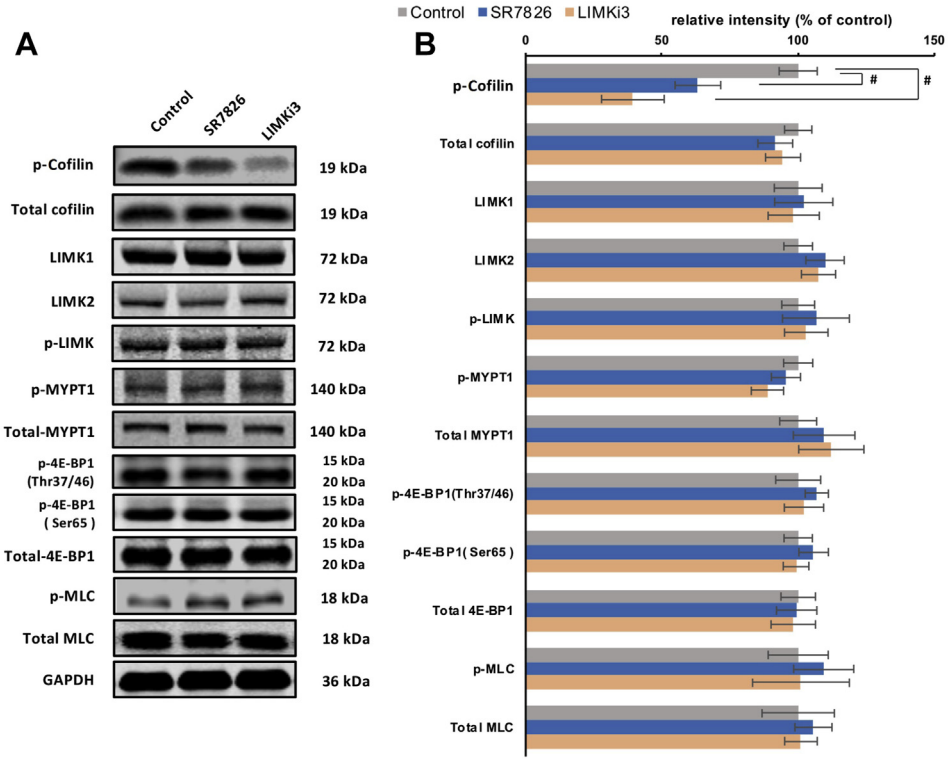

Figure 5 Effects of SR7826 and LIMKi3 on phosphorylation in human bladder smooth muscle cells (HBSMCs). In separate series of experiments, detrusor tissues were incubated with (A) SR7826 (5 μmol/L, 24 h) or DMSO (control), or with (B) LIMKi3 (5 μmol/L, 24 h) or DMSO (control). In the series of SR7826 and DMSO, or LIMKi3 and DMSO, Western blot analyses using site- and phospho-specific antibodies were subsequently performed to compare the phosphorylation states of cofilin, LIMK and MYPT1 (threonine 696), 4E-BP1 (threonine 37/46, serine 65) and MLC between inhibitor and control groups. Values for each sample were calculated as fold of the content of GAPDH and normalized to the mean of the corresponding control group. Data are mean ± SEM from a series of independent experiments ($n = 5$, $^{\#}P < 0.05$ for control *vs.* inhibitor). The preliminary series did not show an informative basis that incubation with inhibitors in 1 μmol/L resulted in changes in cofilin or LIMK phosphorylation, therefore, these series were not continued (data not shown).

3.6. Silencing of LIMK breaks down the actin cytoskeleton and inhibits proliferation in HBSMCs

Transfection of HBSMCs with *LIMK1* and *LIMK2* siRNA caused silencing of LIMK1 and LIMK2 expressions, reflected by decreased levels of *LIMK1* and *LIMK2* mRNA (Fig. 7A), and weaker *LIMK1* and *LIMK2* bands in Western blot analysis compared with HBSMCs transfected with scrambled siRNA, or with wildtype (WT) HBSM cells (Fig. 7B).

Silencing of *LIMK1* and *LIMK2* mimicked the effects of SR7826 and LIMKi3 on actin organization and proliferation observed in EdU assays and phalloidin staining of actin. In HBSMCs transfected with *LIMK1* and *LIMK2* siRNA, less filament organization was observed, and phalloidin staining areas were reduced by 22.2 ± 0.8% and 18.1 ± 1.6% (*LIMK1* siRNA), and 23.8 ± 1.3% and 22.4% ± 1.7% (*LIMK2* siRNA) compared with WT cells and cells transfected with scrambled siRNA, respectively ($P < 0.05$, Fig. 7D).

In the EdU assay, the proliferation rates of HBSMCs transfected with *LIMK1* and *LIMK2* siRNA were reduced by 40.5 ± 2.5% and 37.3 ± 2.7% (*LIMK1* siRNA), and 33.6 ± 2.2% and 34.9 ± 4.9% (*LIMK2* siRNA) compared with WT cells and cells transfected with scrambled siRNA, respectively ($P < 0.05$, Fig. 7E).

3.7. SR7826 and LIMKi3 decrease detrusor contraction and proliferation in vivo

To evaluate effects of BOO on detrusor contents of phospho-cofilin, cofilin, phospho-LIMK, LIMK1, and LIMK2, we established BOO in a rat model by partial ligation of the prostatic urethra for 2 weeks. Western blot analysis revealed that the contents of phospho-cofilin, cofilin, phospho-LIMK, LIMK1, and LIMK2 in BOO detrusors were increased by 82.8 ± 18%, 27.7 ± 2.8%, 107.4 ± 29.5%, 114.3 ± 20.4%, and 83.5 ± 15.6% compared to detrusors of a corresponding sham-operated group, respectively ($P < 0.05$, Fig. 8A). Rats with BOO lasting for 4 weeks showed increased collagen deposition, fibrosis, and diverticula, but decreased percentage of smooth muscle in the bladder by Masson trichrome staining (Supporting Information Fig. S1).

To assess the effects of SR7826 and LIMKi3 on detrusor contractions and proliferation *in vivo*, BOO rats were treated with either SR7826 or LIMKi3 (1 mg/kg·body weight) for 2 weeks. Micturition frequency tests revealed that the micturition frequency of BOO rats was increased by 9.2 ± 0.9 times/2 h compared with sham-operated rats. Treatment of BOO rats with SR7826 or LIMKi3 reduced the micturition frequency by 3.2 ± 0.7 or 7.6 ± 1.3 times/2 h compared with BOO control rats, respectively ($P < 0.05$, Fig. 8B).

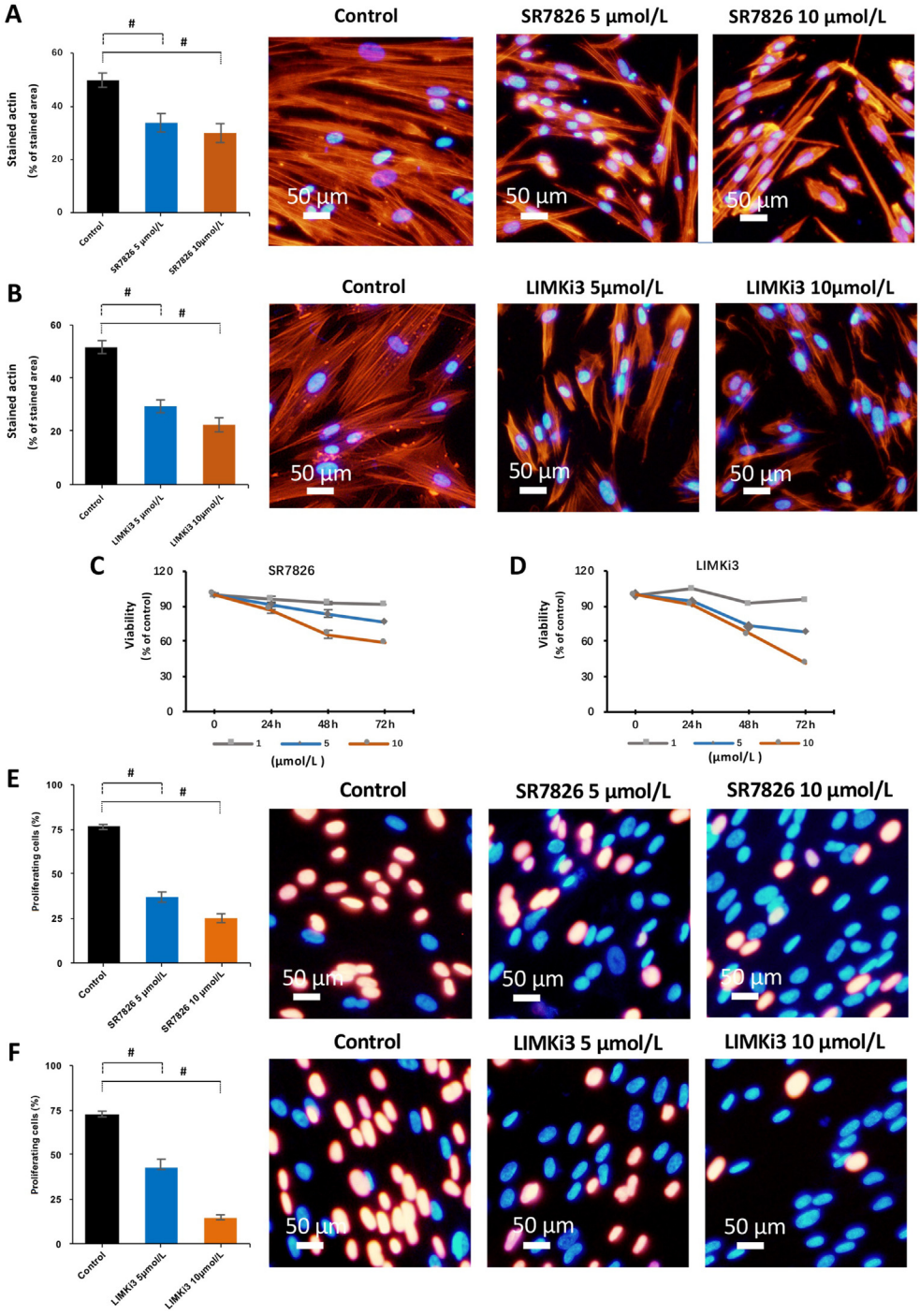

Figure 6 Effects of SR7826 and LIMKi3 on actin filaments, viability and proliferation in human bladder smooth muscle cells (HBSMCs). (A) and (B) HBSMCs were exposed to SR7826 or LIMKi3 at 5 μmol/L or 10 μmol/L for 24 h, or to solvent (DMSO) under the same conditions (controls). Phalloidin staining was used to visualize the polymerized actin. (C) and (D) HBSMCs were exposed to SR7826 or LIMKi3 at 1, 5 or 10 μmol/L for 24, 48, or 72 h, or to solvent (DMSO) under the same conditions (controls). CCK8 was used to analyze the viability of cells in different concentrations and different periods. Viabilities of cells in each concentration and incubation period were treated cells were calculated as fold of the absorbance value in control group were normalized to the mean of the corresponding control cell group. (E) and (F) HBSMCs were exposed to SR7826 or LIMKi3 at 5 or 10 μmol/L for 48 h, or to solvent (DMSO) under the same conditions (controls). An EdU assay was used to assessed for proliferation of cells in different concentrations. Data in (A)−(F) are mean ± SEM from a series of independent experiments ($n = 5$). $^{\#}P < 0.05$ for control *vs.* inhibitor.

Following the micturition frequency tests, bladders were excised and weighted. The bladder weight of BOO control rats was increased by 0.337 ± 0.04 g compared with sham-operated rats, while the bladder weight in BOO rats treated with SR7826 or LIMKi3 was decreased by 0.157 ± 0.03 or 0.187 ± 0.05 g compared with BOO control rats, respectively ($P < 0.05$, Fig. 8C).

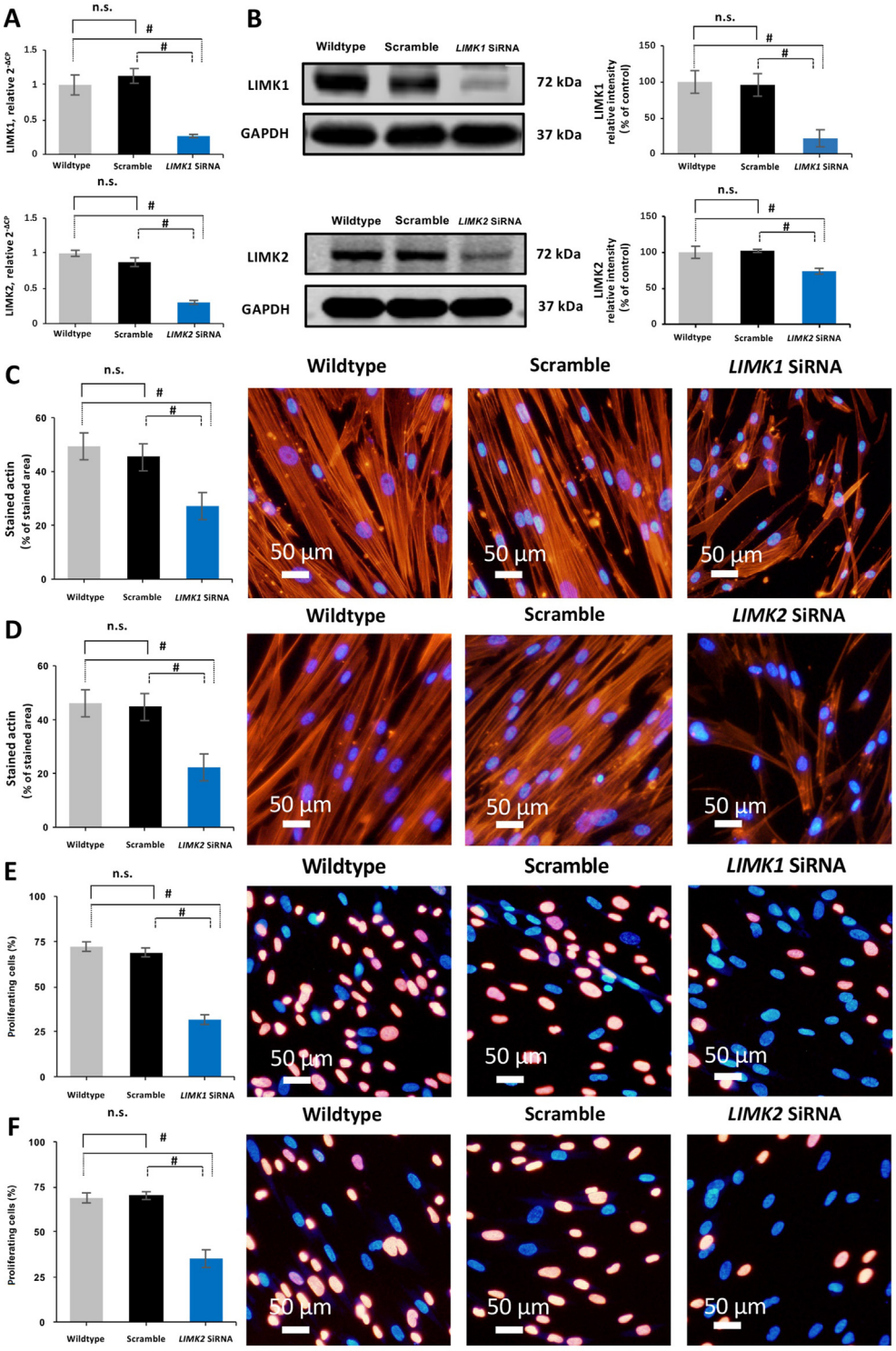

Figure 7 Silencing of *LIMK1* and *LIMK2* expressions in human bladder smooth muscle cells (HBSMCs). (A) and (B) HBSMCs were transfected with scramble siRNA, *LIMK1* siRNA, or *LIMK2* siRNA. The expression of LIMK1 or LIMK2 was compared with cells not being transfected (WT), and with scramble siRNA, respectively. Actin organization by phalloidin staining (C and D), and proliferation by EdU assay (E and F) between WT cells and cells transfected with scramble siRNA, *LIMK1* siRNA, or *LIMK2* siRNA. Data are mean ± SEM from independent experiments in all series ($n = 5$). $^{\#}P < 0.05$ *vs.* WT and scramble; n.s., not significant between WT and scramble.

Changes of detrusor proliferation in the bladder wall were examined by Masson trichrome staining. The stained area was increased by 24.0 ± 1.7% in detrusors of BOO rats compared with sham-operated rats. Treatment of BOO rats with SR7826 or LIMKi3 decreased the stained detrusor area by 27.4 ± 3.8% or 22.2 ± 4.2% compared with BOO control rats, respectively ($P < 0.05$, Fig. 8D). The proliferation of smooth muscle cells in rat bladders was evaluated by PCNA detection.

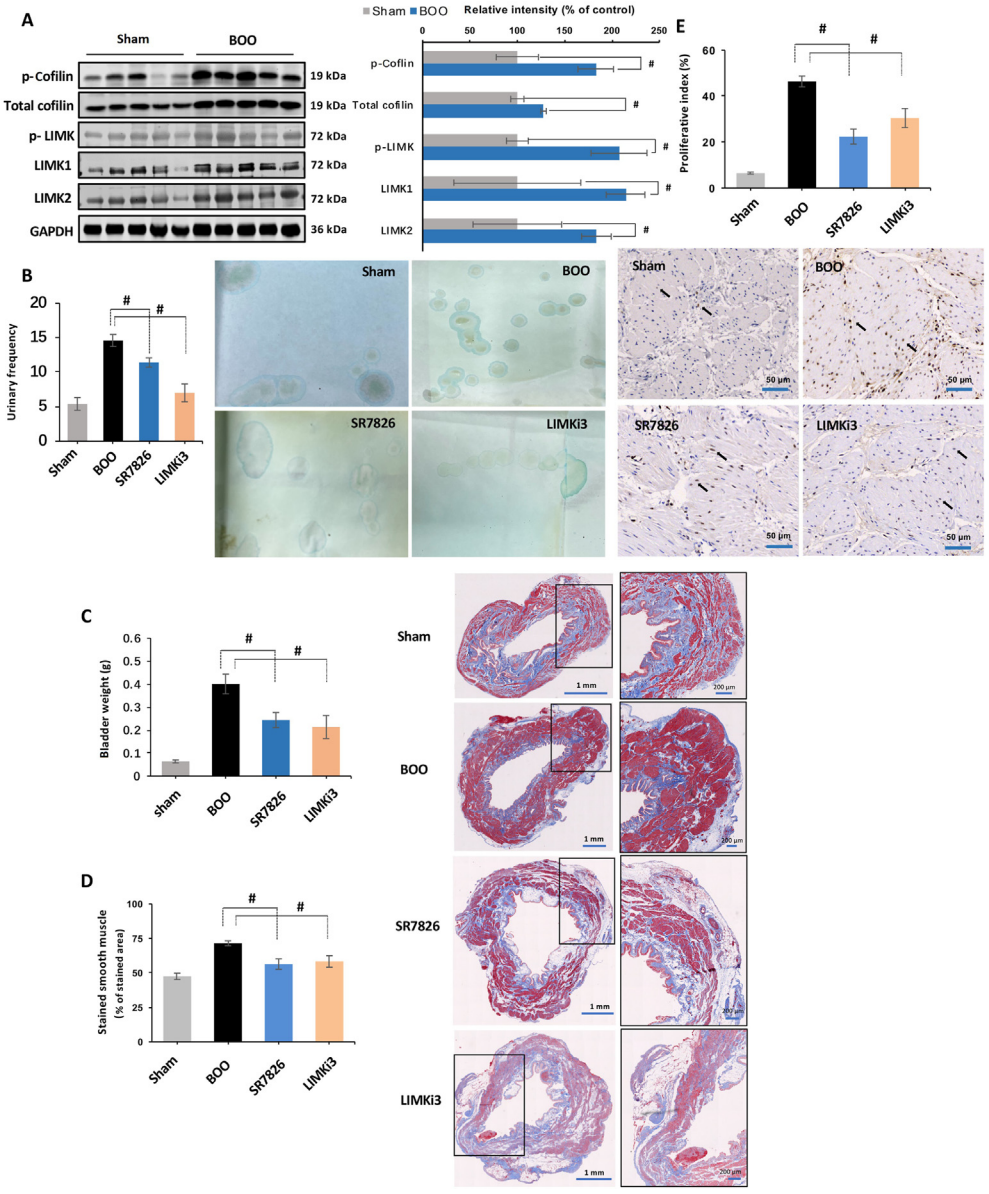

Figure 8 Effects of SR7826 and LIMKi3 on detrusor contractions and proliferation *in vivo*. (A) Bladder outlet obstruction (BOO) in rat was induced by partial ligation on the prostatic urethra for 2 weeks, the contents of phospho-cofilin, cofilin, phospho-LIMK, LIMK1, and LIMK2 were compared with rat without ligation on the prostatic urethra (sham). BOO rats under treatment with SR7826 (1 mg/kg·day, 2 weeks), LIMKi3 (1 mg/kg·day, 2 weeks), or solvent (control), or rat in sham group, were subjected to (B) urinary frequency test by counting the voiding spots in 2 h. (C) Bladder from the experimental rats were weighted, and detrusor tissues were subsequently subjected to (D) Masson trichrome staining to visualize the bladder smooth muscle (stained red) and collagenous fiber (stained blue), or (E) immunohistochemistry analysis to detect the PCNA-positive smooth muscle cells. Data are mean ± SEM from rats ($n = 5$). $^{\#}P < 0.05$ between sham and BOO groups in (A), and $P < 0.05$ for control *vs*. inhibitor treatment in (B)−(E).

Immunohistochemical analyses of detrusor sections revealed an increased percentage of PCNA-positive cells in BOO rats, reflecting an increase of proliferation index, amounting to an increase of 40.0 ± 2.2 percentage points compared with sham-operated rats (Fig. 8E). Treatment of BOO rats with SR7826 or LIMKi3 resulted in a reduction of the proliferation index, amounting to increases of 24 ± 3.3 percentage points or 16 ± 4.1 percentage points compared with BOO control rats, respectively ($P < 0.05$, Fig. 8E).

The lungs, kidneys and livers were excised and stained with HE to visualize histomorphology. Not any impact of LIMK inhibitors on morphology in pulmonary alveolar cells, hepatocytes, or glomeruli was observed (Supporting Information Fig. S2).

4. Discussion

The present study suggests that two structurally unrelated LIMK inhibitors, SR7826 and LIMKi3, effectively inhibit detrusor contraction *in vitro* and *in vivo*. In addition, the *in vivo* experiments in BOO rats proved the bioavailability of both inhibitors. As

far as we can retrieve, this is the first time to report the role of LIMK on promoting smooth muscle contraction in bladder, and the effects of small molecule LIMK inhibitors in bladder. Consequently, our findings may contribute to a more precise understanding of molecular mechanisms in bladder smooth muscle contraction.

SR7826 and LIMKi3 are small molecule inhibitors targeting LIMKs. Cofilin is an important substrate of LIMKs[24]. Consequently, inhibition of cofilin phosphorylation (CP) in detrusor tissues and cells by SR7826 and LIMKi3 may confirm that both inhibitors inhibited LIMK. Although these inhibitory effects were limited to 35%−70%, conclusions explaining the incomplete inhibition by SR7826 and LIMKi3 could not be drawn based on our current data. The possibility of LIMK-independent CP may be taken into consideration; however, as far as we can retrieve, LIMK-independent CP in smooth muscle has not been reported. The N-terminal kinase of testicular protein kinase 1 (TESK1) may be a putative candidate accounting for LIMK-independent CP, as it shows approximately 50% amino acid identity with LIM-kinases[25]. However, its role on CP in smooth muscle is still unclear.

Phosphorylation of LIMK at threonine 508/505 by ROCK or PAK increases its kinase activity to regulate actin dynamics[26,27]. As no reductions of LIMK phosphorylation at this site after treatment with SR7826 and LIMKi3 were observed, we conclude that the effects of LIMK inhibitors on bladder smooth muscle contraction did not rely on this site.

Previous studies reported the promoting effects of phosphorylation of 4E-BP1 and MYPT-1 on detrusor contraction[28,29]. In our present study, we did not observe impacts of SR7826 or LIMKi3 on phosphorylations of 4E-BP1 and MYPT-1, which may suggest the absence or low degree of unspecific kinase inhibition.

Agonist-induced detrusor contraction can be reduced by inhibition of Rho kinase, independently from LIMK[30,31]. Combined application of SR7826/LIMKi3 and Y27632 pointed to possibly separate actions of LIMK and Y27632-inhibited kinases in detrusor contraction in our study. Y27632 was initially reported as a Rho kinase inhibitor, but may inhibit PKA and PKC with K_i values of 25 and 26 μmol/L as well[32]. As we applied 30 μmol/L and considering the additive effects, and involvement of these kinases, and unspecific inhibition of Rho kinase, PKC or PKA by SR7826 or LIMKi3, can be at least partially excluded. Incubation of detrusor tissues with Y27632 did not affect LIMK phosphorylation, indicating that LIMK is no downstream effector of Y27632-inhibited kinases in these tissues. Although serine/threonine kinase 16 (STK16) could be inhibited to 80% by SR7826 at a concentration of 1 μmol/L[33], in a recent study[18], inhibition of the STK16 only slightly inhibited human detrusor contraction. Consequently, the phosphorylation analyses for STK16 substrates were not performed in the present study.

MLC phosphorylation is a key factor in the smooth muscle contraction[34]. In the present study, neither SR7826 nor LIMKi3 affected the MLC phosphorylation in detrusor tissues or HBSMCs, indicating that inhibition of contraction by SR7826 and LIMKi3 was not based on a decrease of MLC phosphorylation. This conclusion may be further supported by our finding that both LIMK inhibitor failed to inhibit KCl-induced detrusor contraction, which involves MLC phosphorylation[35].

Previous studies reported that contractile agonists may change cofilin or LIMK phosphorylation in rat parotid acinar cells[36], outer hair cells[37], and trachea smooth muscle[38]. Also, the thromboxane A2 could increase CP in artery smooth muscle cells[39], human platelets[40], and thymocytes[41]. Similarly, endothelin-1 increases phosphorylation of LIMK and cofilin in ovarian carcinoma cells[42] and artery smooth muscle cells[43]. In the present study, we did not observe changes in LIMK or CP by contractile stimuli including carbachol, acetylcholine or U46619, although inhibitions of their contractions by SR7826 and LIMKi3 were observed. This may suggest that neither muscarinic nor thromboxane receptors activate LIMK in the human bladder. Although the incubation periods of contractile stimuli in theses phosphorylation studies were similar as the periods in organ bath experiments, a transient activation of phosphorylating state escaping out of our time frame may be still possible. However, based on our data, it may be assumed that LIMKs and cofilin constitute a mechanism regulating cholinergic, neurogenic, and thromboxane-induced detrusor contractions under basal conditions, but are not involved in receptor-induced signal transduction to detrusor smooth muscle contraction. Notably, the effects of SR7826 and LIMKi3 were seen, without that grouping of patients for age, history, or clinical background was required, and despite the high individual heterogeneity, which is reflected by variations of marker expression. Together, this may point to a certain relevance of LIMK and cofilin for regulation of detrusor smooth muscle.

In our rat model, increased expression levels of phospho-cofilin, cofilin, phospho-LIMK, LIMK1 and LIMK2 in the bladder were observed, which may reflect crucial roles of these proteins and a possible novel mechanism of bladder smooth muscle contraction, which works independently from muscarinic receptors or β_3-adrenoceptors. Taken together, these results demonstrate that the mechanisms of detrusor contraction are still incompletely understood. Moreover, as SR7826 and LIMKi3 inhibited thromboxane in parallel with muscarinic or neurogenic-induced contraction, better urodynamic effects *in vivo* may be expected than from muscarinic receptor antagonists.

Presently, we cannot explain why both LIMK inhibitors inhibited cholinergic, neurogenic and thromboxane-induced, but not endothelin-induced contractions. Despite the lacking explanation, this finding appears highly interesting, as it points to a generally different regulation of endothelin receptor-induced smooth muscle contraction on the one hand, and of muscarinic or thromboxane receptor-induced contraction in the detrusor on the other. Obviously, LIMK accounts for such differences. In fact, our findings suggesting selective regulation of endothelin-induced contractions in the detrusor may be intriguing, considering that endothelin-1 induces substantial contractions in the human detrusor, what has been only rarely reported for human tissues[44–46], despite the outstanding clinical relevance for detrusor contraction in OAB and LUTS.

Immunoreactivity for phospho-cofilin, LIMK1 and LIMK2 were detected by immunofluorescence in untreated detrusor tissues, which might indicate a pool of active LIMK in the bladder smooth muscle cells. Together with the finding that silencing of LIMK1 and LIMK2 caused breakdown of actin cytoskeleton and reduction of the actin filament in HBSMCs, these results may point to an important role of LIMK as a critical intracellular regulator in bladder smooth muscle contractility. It may be concluded that the LIMK/cofilin pathway may not be activated by muscarinic or TXA_2 receptors agonist to induce bladder smooth muscle contraction, but is able to irregulate contractions by these receptors independently.

In HBSMCs, phalloidin staining suggested that 5 μmol/L of SR7826 and LIMKi3 induce a breakdown of actin cytoskeleton organization. Our findings are in line with previous studies reporting a role of LIMK in actin dynamics in other cell types[16,47].

At 10 μmol/L of SR7826 and LIMKi3, phalloidin staining of actin was less, but still visible. We assume that LIMK-independent CP might be responsible for the incomplete inhibition.

LIMKs have been reported to be involved in progression of several types of cancer including bladder cancer[48], prostate cancer[49], and others[50,51]. In some nonmalignant cell types, a similar role of LIMK has been reported[52,53]. In our EDU assays, both SR7826 and LIMKi3 in 5 μmol/L inhibited proliferation in a concentration-dependent manner, as indicated by decreased number of proliferating cells. Similarly, we observed that silencing of LIMK1 or LIMK2 decreased proliferation in EdU assays, and that treatment with SR7826 or LIMKi3 reduced bladder hypertrophy *in vivo* in BOO rats. These findings may confirm a crucial role of LIMKs in the growth of HBSMCs and in hypertrophy of bladder smooth muscle tissues, so that inhibition of BOO-induced bladder remodeling *in vivo* could therefore be expected.

In the present study, BOO rats treated with SR7826 or LIMKi3 showed a reduced micturition frequency, indicating the relief of OAB symptoms. However, whether this symptom improvement was completely attributed to SR7826/LIMKi3-induced detrusor relaxation may not be concluded from our data. OAB symptoms may also be associated with inflammation in the bladder, while LIMK has been indicated as a regulator during inflammatory processes in some other diseases[54,55]. However, any additional effect of LIMK on the inflammation associated OAB remains unclear, and needs further exploration.

In our BOO rat model, obvious proliferation and hypertrophy in the bladder smooth muscle were observed in the second week of surgery, while increased percentage of collagen deposition, fibrosis, and diverticulum, but decreased percentage of smooth muscle were observed in the fourth week following surgery (Fig. S1). Therefore, and based on the purpose of this study, rats were treated for a period of 2 weeks. The H&E staining of lung, kidney and liver did not reveal toxicities induced by SR7826 or LIMKi3 (Fig. S2), which may suggest a possibly good tolerability of both inhibitors, although toxicity in the long-term applications still need to be further confirmed.

5. Conclusions

The present study indicates that LIMKs promote bladder smooth muscle contraction and proliferation by phosphorylating cofilin and subsequent actin organization. LIMKs play key roles in the BOO-induced OAB. Small molecule LIMK inhibitors, SR7826 and LIMKi3, inhibit smooth muscle contraction and cell proliferation in the human bladder and improve LUTS *in vivo*. A novel pharmacological therapeutic strategy based on LIMKs for the treatment of OAB-related LUTS seems possible.

Acknowledgments

This work was financed by grants from the National Natural Science Foundation of China (Nos. 81900689 and 81870483), and China Postdoctoral Science Foundation (2018M643047).

Author contributions

Qingfeng Yu, Chengjie Wu, Yeda Chen, and Bingsheng Li contributed to the acquisition, analysis and interpretation of data for the work and drafting of the manuscript. Ruixiao Wang, Ru Huang, Di Gu, Xuechun Li, and Xiaolong Wang contributed acquisition of data, analysis and interpretation of data, statistical analysis. Xiaolu Duan, Shujue Li, Yang Liu, and Wenqi Wu contributed analysis and interpretation of data, provided technical or material support. Martin Hennenberg and Guohua Zeng contributed to the conception and design of the work, acquisition, analysis and interpretation of data and drafting of the manuscript.

Conflicts of interest

The authors declare no conflicts of interest.

Appendix A. Supporting information

Supporting data to this article can be found online at https://doi.org/10.1016/j.apsb.2021.01.005.

References

1. Agarwal A, Eryuzlu LN, Cartwright R, Thorlund K, Tammela TL, Guyatt GH, et al. What is the most bothersome lower urinary tract symptom? Individual- and population-level perspectives for both men and women. *Eur Urol* 2014;**65**:1211−7.
2. Noguchi N, Chan L, Cumming RG, Blyth FM, Handelsman DJ, Seibel MJ, et al. Lower urinary tract symptoms and incident falls in community dwelling older men: the concord health and ageing in men project. *J Urol* 2016;**196**:1694−9.
3. Parsons JK, Mougey J, Lambert L, Wilt TJ, Fink HA, Garzotto M, et al. Lower urinary tract symptoms increase the risk of falls in older men. *BJU Int* 2009;**104**:63−8.
4. Van Kerrebroeck PE, Dmochowski R, FitzGerald MP, Hashim H, Norgaard JP, Robinson D, et al. Nocturia research: current status and future perspectives. *Neurourol Urodyn* 2010;**29**:623−8.
5. Stewart WF, Van Rooyen JB, Cundiff GW, Abrams P, Herzog AR, Corey R, et al. Prevalence and burden of overactive bladder in the United States. *World J Urol* 2003;**20**:327−36.
6. Ganz ML, Smalarz AM, Krupski TL, Anger JT, Hu JC, Wittrup-Jensen KU, et al. Economic costs of overactive bladder in the United States. *Urology* 2010;**75**:526−32. 532.e1-18.
7. Fry CH, Meng E, Young JS. The physiological function of lower urinary tract smooth muscle. *Auton Neurosci* 2010;**154**:3−13.
8. Nambiar AK, Bosch R, Cruz F, Lemack GE, Thiruchelvam N, Tubaro A, et al. EAU guidelines on assessment and nonsurgical management of urinary incontinence. *Eur Urol* 2018;**73**:596−609.
9. Andersson KE. Muscarinic acetylcholine receptors in the urinary tract. *Handb Exp Pharmacol* 2011;(202):319−44.
10. Sexton CC, Notte SM, Maroulis C, Dmochowski RR, Cardozo L, Subramanian D, et al. Persistence and adherence in the treatment of overactive bladder syndrome with anticholinergic therapy: a systematic review of the literature. *Int J Clin Pract* 2011;**65**:567−85.
11. Mitcheson HD, Samanta S, Muldowney K, Pinto CA, Rocha BA, Green S, et al. Vibegron (RVT-901/MK-4618/KRP-114V) administered once daily as monotherapy or concomitantly with tolterodine in patients with an overactive bladder: a multicenter, phase IIb, randomized, double-blind, controlled trial. *Eur Urol* 2019;**75**:274−82.
12. Li B, Yu Q, Wang R, Gratzke C, Wang X, Spek A, et al. Inhibition of female and male human detrusor smooth muscle contraction by the Rac inhibitors EHT1864 and NSC23766. *Front Pharmacol* 2020;**11**:409.
13. Rahnama'i MS, van Kerrebroeck PE, de Wachter SG, van Koeveringe GA. The role of prostanoids in urinary bladder physiology. *Nat Rev Urol* 2012;**9**:283−90.
14. Han JH, Lee MY, Myung SC. The effect of endothelin-1 on the production of interleukin-6 in cultured human detrusor smooth

muscle cells, and the effect of interleukin-6 on the contractile response of bladder smooth muscle strips from rats. *BJU Int* 2009;**104**:707−12.
15. Hennenberg M, Kuppermann P, Yu Q, Herlemann A, Tamalunas A, Wang Y, et al. Inhibition of prostate smooth muscle contraction by inhibitors of Polo-like kinases. *Front Physiol* 2018;**9**:734.
16. Bernard O. Lim kinases, regulators of actin dynamics. *Int J Biochem Cell Biol* 2007;**39**:1071−6.
17. Yu Q, Gratzke C, Wang Y, Herlemann A, Sterr CM, Rutz B, et al. Inhibition of human prostate smooth muscle contraction by the LIM kinase inhibitors, SR7826 and LIMKi3. *Br J Pharmacol* 2018;**175**:2077−96.
18. Li B, Wang X, Rutz B, Wang R, Tamalunas A, Strittmatter F, et al. The STK16 inhibitor STK16-IN-1 inhibits non-adrenergic and non-neurogenic smooth muscle contractions in the human prostate and the human male detrusor. *Naunyn-Schmiedeberg's Arch Pharmacol* 2020;**393**:829−42.
19. Yu Q, Gratzke C, Wang R, Li B, Kuppermann P, Herlemann A, et al. A NAV2729-sensitive mechanism promotes adrenergic smooth muscle contraction and growth of stromal cells in the human prostate. *J Biol Chem* 2019;**294**:12231−49.
20. Melman A, Tar M, Boczko J, Christ G, Leung AC, Zhao W, et al. Evaluation of two techniques of partial urethral obstruction in the male rat model of bladder outlet obstruction. *Urology* 2005;**66**:1127−33.
21. Wang J, Chen Y, Gu D, Zhang G, Chen J, Zhao J, et al. Ketamine-induced bladder fibrosis involves epithelial-to-mesenchymal transition mediated by transforming growth factor-β1. *Am J Physiol Ren Physiol* 2017;**313**:F961−72.
22. Song B, Jiang W, Alraies A, Liu Q, Gudla V, Oni J, et al. Bladder smooth muscle cells differentiation from dental pulp stem cells: future potential for bladder tissue engineering. *Stem Cell Int* 2016;**2016**:6979368.
23. Baskin LS, Hayward SW, Sutherland RA, DiSandro MJ, Thomson AA, Goodman J, et al. Mesenchymal−epithelial interactions in the bladder. *World J Urol* 1996;**14**:301−9.
24. Arber S, Barbayannis FA, Hanser H, Schneider C, Stanyon CA, Bernard O, et al. Regulation of actin dynamics through phosphorylation of cofilin by LIM-kinase. *Nature* 1998;**393**:805−9.
25. Sarmiere PD, Bamburg JR. Regulation of the neuronal actin cytoskeleton by ADF/cofilin. *J Neurobiol* 2004;**58**:103−17.
26. Edwards DC, Sanders LC, Bokoch GM, Gill GN. Activation of LIM-kinase by Pak1 couples Rac/Cdc42 GTPase signalling to actin cytoskeletal dynamics. *Nat Cell Biol* 1999;**1**:253−9.
27. Ohashi K, Nagata K, Maekawa M, Ishizaki T, Narumiya S, Mizuno K. Rho-associated kinase ROCK activates LIM-kinase 1 by phosphorylation at threonine 508 within the activation loop. *J Biol Chem* 2000;**275**:3577−82.
28. Juan YS, Li S, Levin RM, Kogan BA, Schuler C, Leggett RE, et al. The effect of ischemia/reperfusion on rabbit bladder—role of Rho-kinase and smooth muscle regulatory proteins. *Urology* 2009;**73**:1126−30.
29. Anjum I. Calcium sensitization mechanisms in detrusor smooth muscles. *Clin Physiol Pharmacol* 2018;**29**:227−35.
30. Dér B, Molnár PJ, Ruisanchez É, orsy P, Kerék M, Faragó B, et al. NK2 receptor-mediated detrusor muscle contraction involves $G_{q/11}$-dependent activation of voltage-dependent Ca^{2+} channels and the RhoA-Rho kinase pathway. *Am J Physiol Ren Physiol* 2019;**317**:F1154−63.
31. Boberg L, Poljakovic M, Rahman A, Eccles R, Arner A. Role of Rho-kinase and protein kinase C during contraction of hypertrophic detrusor in mice with partial urinary bladder outlet obstruction. *BJU Int* 2012;**109**:132−40.
32. Uehata M, Ishizaki T, Satoh H, Ono T, Kawahara T, Morishita T, et al. Calcium sensitization of smooth muscle mediated by a Rho-associated protein kinase in hypertension. *Nature* 1997;**389**:990−4.
33. Yin Y, Zheng K, Eid N, Howard S, Jeong JH, Yi F, et al. Bis-aryl urea derivatives as potent and selective LIM kinase (Limk) inhibitors. *J Med Chem* 2015;**58**:1846−61.
34. Morano I. Tuning smooth muscle contraction by molecular motors. *J Mol Med (Berl)* 2003;**81**:481−7.
35. Ratz PH, Berg KM, Urban NH, Miner AS. Regulation of smooth muscle calcium sensitivity: KCl as a calcium-sensitizing stimulus. *Am J Physiol Cell Physiol* 2005;**288**:C769−83.
36. Takuma T, Ichida T, Yokoyama N, Tamura S, Obinata T. Dephosphorylation of cofilin in parotid acinar cells. *J Biochem* 1996;**120**:35−41.
37. Matsumoto N, Kitani R, Maricle A, Mueller M, Kalinec F. Pivotal role of actin depolymerization in the regulation of cochlear outer hair cell motility. *Biophys J* 2010;**99**:2067−76.
38. Zhao R, Du L, Huang Y, Wu Y, Gunst SJ. Actin depolymerization factor/cofilin activation regulates actin polymerization and tension development in canine tracheal smooth muscle. *J Biol Chem* 2008;**283**:36522−31.
39. Fediuk J, Gutsol A, Nolette N, Dakshinamurti S. Thromboxane-induced actin polymerization in hypoxic pulmonary artery is independent of Rho. *Am J Physiol Lung Cell Mol Physiol* 2012;**302**:L13−26.
40. Iida Y, Doi T, Tokuda H, Matsushima-Nishiwaki R, Tsujimoto M, Kuroyanagi G, et al. Rho-kinase regulates human platelet activation induced by thromboxane A2 independently of p38 MAP kinase. *Prostaglandins Leukot Essent Fatty Acids* 2015;**94**:73−81.
41. Harenberg A, Girkontaite I, Giehl K, Fischer KD. The Lsc RhoGEF mediates signaling from thromboxane A2 to actin polymerization and apoptosis in thymocytes. *Eur J Immunol* 2005;**35**:1977−86.
42. Semprucci E, Tocci P, Cianfrocca R, Sestito R, Caprara V, Veglione M, et al. Endothelin A receptor drives invadopodia function and cell motility through the β-arrestin/PDZ-RhoGEF pathway in ovarian carcinoma. *Oncogene* 2016;**35**:3432−42.
43. Weise-Cross L, Sands MA, Sheak JR, Broughton BRS, Snow JB, Gonzalez Bosc LV, et al. Actin polymerization contributes to enhanced pulmonary vasoconstrictor reactivity after chronic hypoxia. *Am J Physiol Heart Circ Physiol* 2018;**314**:H1011−21.
44. Zhang X, Kuppam DS, Melman A, DiSanto ME. *In vitro* and *in vivo* relaxation of urinary bladder smooth muscle by the selective myosin II inhibitor, blebbistatin. *BJU Int* 2011;**107**:310−7.
45. Uckert S, Stief CG, Lietz B, Burmester M, Jonas U, Machtens SA. Possible role of bioactive peptides in the regulation of human detrusor smooth muscle—functional effects *in vitro* and immunohistochemical presence. *World J Urol* 2002;**20**:244−9.
46. Okamoto-Koizumi T, Takeda M, Komeyama T, Hatano A, Tamaki M, Mizusawa T, et al. Pharmacological and molecular biological evidence for ETA endothelin receptor subtype mediating mechanical responses in the detrusor smooth muscle of the human urinary bladder. *Clin Sci (Lond)* 1999;**96**:397−402.
47. Antonipillai J, Rigby S, Bassler N, Peter K, Bernard O. Pharmacological inhibition of LIM kinase pathway impairs platelets functionality and facilitates thrombolysis. *Exp Cell Res* 2019;**382**:111458.
48. Wang W, Yang C, Nie H, Qiu X, Zhang L, Xiao Y, et al. LIMK2 acts as an oncogene in bladder cancer and its functional SNP in the microRNA-135a binding site affects bladder cancer risk. *Int J Cancer* 2019;**144**:1345−55.
49. Mardilovich K, Gabrielsen M, McGarry L, Orange C, Patel R, Shanks E, et al. Elevated LIM kinase 1 in nonmetastatic prostate cancer reflects its role in facilitating androgen receptor nuclear translocation. *Mol Cancer Therapeut* 2015;**14**:246−58.
50. Lee MH, Kundu JK, Chae JI, Shim JH. Targeting ROCK/LIMK/cofilin signaling pathway in cancer. *Arch Pharm Res (Seoul)* 2019;**42**:481−91.
51. Chen J, Ananthanarayanan B, Springer KS, Wolf KJ, Sheyman SM, Tran VD, et al. Suppression of LIM kinase 1 and LIM kinase 2 limits glioblastoma invasion. *Cancer Res* 2020;**80**:69−78.

52. Wen Z, Han L, Bamburg JR, Shim S, Ming GL, Zheng JQ. BMP gradients steer nerve growth cones by a balancing act of LIM kinase and Slingshot phosphatase on ADF/cofilin. *J Cell Biol* 2007;**178**:107−19.
53. Wang W, Townes-Anderson E. LIM kinase, a newly identified regulator of presynaptic remodeling by Rod photoreceptors after injury. *Invest Ophthalmol Vis Sci* 2015;**56**:7847−58.
54. Hu F, Liu HC, Su DQ, Chen HJ, Chan SO, Wang Y, et al. Nogo-A promotes inflammatory heat hyperalgesia by maintaining TRPV-1 function in the rat dorsal root ganglion neuron. *FASEB J* 2019;**33**:668−82.
55. Tong H, Qi D, Guan X, Jiang G, Liao Z, Zhang X, et al. c-Abl tyrosine kinase regulates neutrophil crawling behavior under fluid shear stress *via* Rac/PAK/LIMK/cofilin signaling axis. *J Cell Biochem* 2018;**119**:2806−17.